Lab on a Chip

Disposable surface plasmon resonance aptasensor with membrane-based sample handling design for quantitative interferon-gamma detection

Journal:	*Lab on a Chip*
Manuscript ID:	LC-ART-02-2014-000249.R1
Article Type:	Paper
Date Submitted by the Author:	22-Apr-2014

Complete List of Authors:	Chuang, Tsung-Liang; National Taiwan University, Institute of Biomedical Engineering Chang, Chia-Chen; National Taiwan University, Institute of Biomedical Engineering Chu-Su, Yu; National Taiwan University, Institute of Biomedical Engineering Wei, Shih-Chung; National Taiwan University, Graduate Institute of Biology Electronics and Bioinformatics Zhao, Xihong; National Taiwan University, Institute of Biomedical Engineering Hsueh, Po-Ren; National Taiwan University, Department of LaboratoryMedicine Lin, Chii-Wann; National Taiwan University, Institute of Biomedical Engineering

SCHOLARONE™
Manuscripts

Table of Contents Entry

Membrane based microfluidic device integrated the surface plasmon resonance sensor was used for interferon-gamma detection, with the availability of quantitative experimental processes.

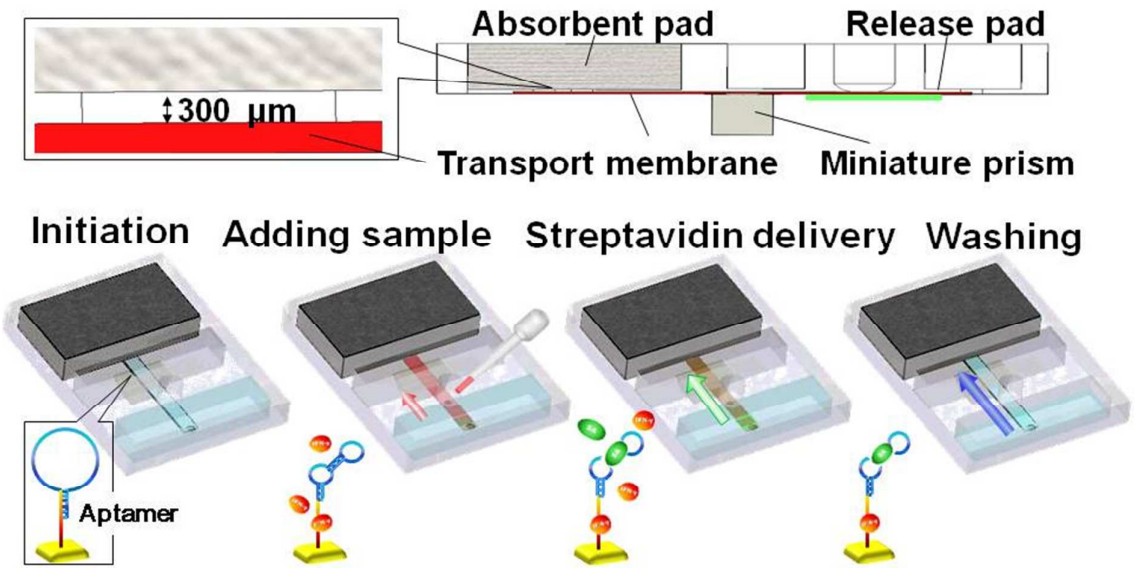

Lab on a Chip

Disposable surface plasmon resonance aptasensor with membrane-based sample handling design for quantitative interferon-gamma detection

Journal:	*Lab on a Chip*
Manuscript ID:	LC-ART-02-2014-000249.R1
Article Type:	Paper
Date Submitted by the Author:	n/a

Complete List of Authors:	Chuang, Tsung-Liang; National Taiwan University, Institute of Biomedical Engineering Chang, Chia-Chen; National Taiwan University, Institute of Biomedical Engineering Chu-Su, Yu; National Taiwan University, Institute of Biomedical Engineering Wei, Shih-Chung; National Taiwan University, Graduate Institute of Biology Electronics and Bioinformatics Zhao, Xihong; National Taiwan University, Institute of Biomedical Engineering Hsueh, Po-Ren; National Taiwan University, Department of LaboratoryMedicine Lin, Chii-Wann; National Taiwan University, Institute of Biomedical Engineering

SCHOLARONE™
Manuscripts

Disposable surface plasmon resonance aptasensor with membrane-based sample handling design for quantitative interferon-gamma detection

Tsung-Liang Chuang[1], Chia-Chen Chang[1], Yu Chu-Su[1], Shih-Chung Wei[2], Xi-hong Zhao[1], Po-Ren Hsueh[3], Chii-Wann Lin [1,4*]

1. Institute of Biomedical Engineering, National Taiwan University, Taipei,10617,Taiwan
2. Institute of Biology Electronics and Bioinformatics National Taiwan University, Taipei, 10617, Taiwan
3. Department of Laboratory Medicine, National Taiwan University, Taipei 10051, Taiwan
4. Center for Emerging Material and Advanced Devices, National Taiwan University, Taipei, 10617, Taiwan

Tel.: +886 2 33665271, E-mail address: cwlinx@ntu.edu.tw

Abstract

ELISA and ELISPOT methods are utilized for interferon-gamma (IFN-γ) release assays (IGRAs) to detect the IFN-γ secreted by T lymphocytes. However, the multi-step protocols of the assays are still performed with laboratory instruments and operated by well-trained people. Here, we report a membrane-based microfluidic device integrated with a surface plasmon resonance (SPR) sensor to realize an easy-to-use and cost effective multi-step quantitative analysis. To conduct the SPR measurements, we provided a membrane-based SPR sensing device in which a rayon membrane located 300 μm under the absorbent pad. The basic equation covering this type of transport is based on Darcy's law. Furthermore, the concentration of streptavidin delivered from sucrose-treated glass pad placed alongside the rayon membrane was controlled in a narrow range (0.81 μM $\pm$ 6%) . Finally, the unbound molecules were removed by a washing buffer that was pre-packed in the reservoir of the chip. Using a bi-functional, hairpin-shaped aptamer as the sensing probe, we specifically detected the IFN-γ and amplified the signal by binding the streptavidin A high correlation coefficient (R^2 = 0.995) was obtained, in the range from 0.01 to 100 nM. The detection limit of 10 pM was achieved within 30 min. Thus, the SPR assay protocols for IFN-γ detection could be performed using this simple device without an additional pumping system.

Introduction

Due to the global aging and ineffectiveness of tuberculosis (TB) drugs[1], *mycobacterium tuberculosis (MTB)* is a re-emerging worldwide public health problem[2]. However, the symptomless latent TB infection is still a major concern for high-risk populations, such as health care workers (HCWs)[3], HIV-positive patients, and immigrants, even in developed countries[4]. The tuberculin skin test (TST) and interferon gamma (IFN-γ) release assays (IGRAs) are considered appropriate methods for testing for TB. The TST method can be easily applied in low-resource environments[5]. However, it is influenced by the Bacille Calmette-Guérin (BCG) vaccination and *nontuberculous mycobacteria* (NTM)[6]. Thus, IGRAs have been viable alternative diagnosis tools due to their sensitivity and specificity[7]. In brief, the existing approach for latent TB diagnosis based on IGRAs is to determine the amount of IFN-γ produced from T cells that have been stimulated with added antigen, such as early secretary antigen target 6 (ESAT-6) and culture filtrate protein 10 (CFP-10)[8,9], through ELISA or ELISPOT assays[10]. The application of technologies are still confined due to the direct cost of the device itself and the associated costs of the operational personnel and required equipment, particularly for areas with limited resources. Twenty-four hours, as well as the appropriate culture resources and manpower, are required to produce an appropriate amount of IFN-γ in the culture medium. In addition, these assays are still constrained by indeterminate results, which can result from manual measurement processes, such as vortexing before incubation and labeling and washing steps[11]. The existing IGRA-based commercial tools require costly devices that provide semi-quantitative results and are limited to analytical laboratories. Therefore, the development of a quantitative IFN-γ system that is integrated with the benefits of a low detection limit, high sensitivity, cost

effectiveness, and an ease of use in medical applications for resource-limited settings is essential.

Compared with antibody-based immunoassays, aptamers are amenable to in vitro synthesis and more tolerant under detrimental environment. Hence, aptamers have been integrated with different transducer and exploited to fabricate biosensors in various applications (e.g. diagnosis, food industry and environmental monitoring)[12]. Mass sensitive biosensor with the real-time and label-free advantages has constructed using both quartz crystal microbalance (QCM) and surface plasmon resonance (SPR). QCM immunosensor has been successfully used for the measurement of insulin[13] and carbohydrate antigen 15-3 (CA15-3) [14] in the buffer solution and SPR biosensor for retinol binding protein 4 (RBP4) in the serum[15]. Compared with the QCM biosensor, the SPR-based biosensor[16] is flexible to integrate with different liquid handling systems operated in the laboratory[17], such as flow cells, cuvettes, and microfluidic (bio) chips. Furthermore, to enhance the sensitivity, a bi-functional structure switching aptamer SPR sensor for sequentially binding to INF-γ and streptavidin has been demonstrated in the plasma[18].

For increasing the practicality of point-of-care application, the different technique had been integrated in an assay, such as surface acoustic waves (SAW)[19], and membrane based platforms. The SAW platform, could flexibly handle nanoliter-sized volumes of liquid droplets on a hydrophobic surface with a piezoelectric chip. However, the programmability required additional control system and is based on the complex designs of the interdigital electrodes and the hydrophobic/hydrophilic areas. In addition, the long term stability of these hydrophobic and hydrophilic surface coatings is another challenge for practical application. Unlike SAW platform, the characteristics of membrane based microfluidic device are simple and flexible to design and could be seen as robustness and the implemented lab-on-a-chip application[20] . Nitrocellulose strips integrated with waveguide SPR immunosensor

was developed to analyze the avian leukosis virus (ALV) specimens as a prototype for portable applications[21]. To perform the laboratory operation protocols without additional equipment, a membrane-based microfluidic device was designed that employed a plastic structure and various membranes with different size and treatments to operate the SPR aptasensor and quantify chemicals.

Membrane-based fluidic devices have been widely used in diagnostic fields due to their simplicity, uncomplicated construction, and relative cost effectiveness. For instance, a lateral-flow test (LFT) could provide a set of fluidic unit operations[22] for a pregnancy test or chromatographic immunoassay (CIA) that directly detected the TB antibody (ex. anti-MPB64 monoclonal antibody)[23] in human serum or plasma specimens. Many advanced techniques have been created to expand the function of lateral flow devices. A 2D paper network (2DPN) platform could be used to perform multistep processing[24–27] and improve the limit of detection [28]. A.W. Martinez provided the paper device in which three-dimensional patterns were stacked to link a single inlet with multiple detection regions[29]. Although this device is easy to use, its use is still challenging in SPR measurements. For example, after the assay process scheme was performed through capillary force, the propagation of liquid could not be stopped before the absorbent pad was fully wetted with liquid and the flow rate is hard to control. Second, the concentration of the reagent that was pre-storage in a released pad will be strongly affected by variations in the amount of aqueous sample. In addition, uncontrolled liquid evaporation causes a variety in the moisture content of the porous membranes. Thus, the sample-handing process of SPR assays is hard to perform in the existing lateral flow- or paper-based device.

In this paper, we provide a paper based microfluidic device that absorbent pad and transport membrane was separated to satisfy the operational processes of SPR detection for IFN-γ endpoint analysis. The sample handling process includes transporting the sample solution through the detection surface and then stopping flow,

releasing the streptavidin as the molecule in the signal amplification, and washing out the unbound sample, as shown in Fig. 1. Furthermore, the membrane-based microfluidic device also autonomously applied the quantitative reagent (*e.g.*, a desired concentration of streptavidin) to the detection region for enhancing the IFN-γ signal based on SPR technique without an external driving system. Finally, the device could maintain moisture content of the transport membrane during the measurement.

Results and Discussion

Surface plasmon resonance instrument

To integrate this system, we attempted to achieve a state-of-the-art performance and avoid a complicated and expensive construction. A simple and effective SPR instrument was constructed in the study. The (850 ± 50 nm) LED (EDEI-1 LA3, EDISON OPTO, Taiwan); the plano-convex lens set and polarizer were compacted into the incident arm as a light source for excitation of the SPR. This collimated light beam was aligned toward the cyclic olefin copolymer (COC) prism at an appropriate angle of 67°. A plate holder was used to conveniently place the sensing plate in the desired position on the optical path to allow for the reflection of light to be projected to a camera via an industrial lens (TV LENS 12 MM 1: 1.4, Japan). For quantitative comparison, all of the gray-scale pixels in the regions of interest (ROIs) were averaged, yielding the response units (RUs). We have observed a difference of 2,500 response unit (ΔRU) between the SPR maximum signal (2,700 RU) and the minimum signal (200 RU). The reflected light intensity was affected by the amount of the IFN-γ that interacted with the immobilized aptamers on the gold surface. We obtained a measure of the IFN-γ-aptamer interaction by detecting the changes in the intensity of the reflected light.

Configuration of the autonomous process sensing cartridge

In the 3D membrane configuration, based upon the COC fluidic cartridge, the fluid flow through the detection region was driven by capillary action from the transport membrane and absorbent pad, as shown in Fig. 2B. The following special designs made our sample sensing cartridge different from that of the traditional lateral flow devices and capillary-based microfluidic processing device.

In the device, our inlet was higher than the outlet. The pressure resulting from the height difference provided an additional driving force for the aqueous sample. This pressure difference aids in the rapid penetration of the sample liquid through the transport membrane (2.5 × 30 mm) and aids in the ability of the sample liquid to overcome the outlet barrier between the absorbent pad and transport membrane (as shown in Fig. 2B). The location of the absorbent pad is different from the traditional design, in which the absorbent pad is connected to the transport membrane (or strip paper); in contrast, the absorbent pad in the new device does not possess direct contact with the transport membrane directly but is instead situated 300 μm above the transport membrane, as show in Fig. 2B. Furthermore, the rayon membrane that was packed in the micro-channel was used to transport the aqueous sample and retain a certain amount of the sample solution in the micro-channel, as shown in Fig. 3c. These design modifications allow a constant sample volume to be trapped in the transport membrane before the saturation of the absorbent pad while retaining the controlled propulsion of the sample solution propulsion in the membrane without a saturated absorbent pad. The rayon-based, spunlace, nonwoven membrane was used as the transport membrane due to its high degree of hydrophilicity and porousness. The properties of the rayon-based transport membrane can contribute high-speed transport (0.5-1 cm/s) and good absorptivity to accelerate processing. The buffer solution for the released pad is well known[30]. In briefly, the borate

provides the stability of the pH value and slightly enhances the dissolved particles. The sucrose serves as a preservative and as a re-solubilization agent for the dry reagent (*i.e.*, streptavidin). When bio-molecules are dried with sucrose, the sucrose molecules form a matrix around the particles to stabilize the biological structures. When the sample enters the pad, the sugar molecules instantaneously dissolve, carrying the biological particles away from the surface and into the fluid stream.

Functional verification of autonomous processing for SPR detection

Here, we utilized various color solutions to visualize the liquid handling processes in the membrane-based microfluidic device to satisfy the operational procedures of the SPR detection via the different color solutions. As shown in Fig. 3b, the sample (red color) was added to the sample well in excess and allowed to flow into the transport membrane, and the excess sample was discharged and absorbed by the absorbent pad at the outlet. This discharge process occurred for 10-30 s until a balance in pressure was achieved. Fig. 3c demonstrates that a certain amount of sample (red color solution) remained in the flow channel and that the absorbent pad had not been completely saturated. This device is different from a traditional paper-based device in that liquid was wicked by the absorbent pad until a hydroscopic balance was attained. The basis of the model is most commonly used to describe flow in a capillary or porous medium. The basic equation covering this type of transport is Darcy's law, which can be written as

$$Q = -\frac{\kappa wh}{\eta L}\Delta P$$

where Q is the volumetric flow rate, κ is the permeability of the paper, wh is the paper cross-sectional area of width w and height h, η is the dynamic viscosity, and ΔP is the pressure drop occurring over the length L of the membrane[26]. For this work, we assume that the intrinsic characteristics of the membrane material, κ, w, and h, are

constant and that the aqueous samples possess the same viscosity, η. The volumetric flow rate in the paper devices is controlled by the pressure. Therefore, the fluidic flow in the rayon paper can be stopped when a balance in pressure has been attained between the fluid source and sink. In Fig. 3d, green dye that had been dried in the released pad was dissolved by the sample solution that had been released from the release pad after it has passed through the transport membrane. This design prevented the sample fluid from removing the dried reagents on the release pad out of the transport membrane, thus maintaining a relatively constant reagent concentration. For shortening the processes time, the green dye solution didn't contain sucrose. The duration of sample standing in the transport membrane could be determined depended on the experimental needs. Fig. 3f illustrates the washing step, which was carried out by breaking the thin film covering the buffer solution tank. The color dye was removed from the transport membrane by washing with the buffer solution, as shown Fig. 3g. As shown in Fig. 3h, the waste liquid was absorbed by the absorbent pad. Here, we activated the washing step manually with soldering guns. Whereas the washing solution flowed through the transport membrane, the red and green color solutions were both carried off, as shown in Figs. 3g and 3h. As illustrated above, the membrane based micro-fluidics can provide a simple and robust function for uncomplicated process of liquid operation without additional control system.

Stability of the streptavidin concentration with different sample addition volumes

Here, we demonstrated that the concentration of streptavidin in the transport membrane was not influenced by changes in the amount of sample added. Because the SPR signal could only respond to a change in the effective refractive index, which could correlate with the concentration of the reagent or be due to a binding reaction between the aptamers and analytes, deionized distilled water was used as the

sample solute to avoid a signal contribution from the binding reaction between the analytes. The SPR response due to the streptavidin solution was 52.371 ΔRU. After the addition of 20, 40, 60, and 80 μl of the sample, the average SPR responses of the rehydrated streptavidin from the measurements in triplicate were 21.37, 20.97, 21.42, and 20.78ΔRU, respectively, yielding streptavidin concentrations of 0.816, 0.80, 0.818, and 0.79 μM, respectively as show in fig. 4. This experimental result indicated that the design limited the fluctuation of the streptavidin concentration to a narrow range (0.81 μM ± 6%) and that the concentration was not diluted when additional solution was added. The design for maintaining the concentration of a reagent in a narrow range was based on two factors. First, a certain amount of the sample could be reserved in the micro-channel that contained the transport membrane, as discussed in section 3.4. Second, the reagent can be delivered with a time delay. For that purpose, we added a streptavidin solution that included sucrose in the releasing pad to slow the release of the streptavidin. The phenomenon regarding the inclusion of the sugar has been thoroughly discussed in previous study[32]. Briefly, the wicking rate of the strip is controlled by the fluid viscosity, to which the dissolved sucrose contributes, and can be calculated via the Lucas–Washburn (L-W) equation. The releasing pad was located in the opposite direction of the sample discharge 25 mm away from the outlet. The design of this space barrier could avoid the early removal of the reagent from the transport membrane through an early discharge process. The stability of the concentration of the streptavidin in the transport membrane is critical for the endpoint analysis based on SPR detection. Thus, we demonstrated that the design could prevent the change in streptavidin concentration resulting from adding various amounts of sample. Our results demonstrated that the dried streptavidin added to the released pad could be rehydrated and used to control the concentration in the desired narrow range without controlling the amount of sample added. The biological activity could be maintained

and promoted for the extended retention time because the reagent was stored in the release pad in a dried form. For point-of-care application, the user could add volumes without the use of pipettes.

SPR-based analysis for the multi-step process sensing cartridge

Fig. 5 presents the time series data collected through the SPR technique that indicated the various stages in the multi-step process shown in Fig. 3. In the initial step, a small amount of the washing solution (8 μl) was allowed into the transport membrane for 1 min; meanwhile, the SPR signal (ΔRU) responded to the bulk refractive index of the washing solution, which was used as the baseline. After the sample was added manually, the refractive index increased rapidly with time due to the changes of bulk refractive index in the refractive index between the sample solution and buffer and approached the first plateau (122.7 ΔRU) in 16-20 s. The first plateau indicated that the bulk refractive index near the detection region did not change, possibly because the aqueous sample flow had stopped and remained in the transport membrane, particularly with the limited amount of the sample. After the plateau had been maintained for a period of time (~75 s), the streptavidin-sugar solution that had been dried on the released pad was dissolved by the aqueous sample into the transport membrane and the SPR signal increased again, as shown in Fig. 4. The dried sugar solutions in the porous medium were utilized for providing time delays to deliver the reagent[27]. In this study, we supplied streptavidin as the signal amplifier proteins when the aqueous sample stopped flowing in the membrane to prevent the streptavidin reagents from being carried off during the discharging of the sample. When the washing step was activated manually by breaking the thin film cover on the buffer solution bank, the sample solution that contained the unbound IFN-γ, streptavidin, and other reagents was removed, and the signal decreased rapidly and reached a plateau (22.3 ΔRU). This difference in signal response

indicated that the IFN-γ and streptavidin molecules bonded with the aptamers that were immobilized on the gold surfaces. The total time required for the utilization of this device is less than the total time required for a similar experiment on a bench-based experimental setup, as demonstrated in our previous study. Our COC prism has the advantage of a direct gold film deposition without an additional adhesive layer between the substrate and the gold film. It thus provides a simpler and cheaper fabrication process. We integrated the COC prism with the microfluidic handling cartridge without using matching oils for the coupling of a gold glass slide and an optical prism, as required by the traditional SPR operation approach. Thus, the operation process can be further simplified, and the cost of materials for these disposable applications can be reduced. The SPR instrument does not include the breaking apparatus. The SPR system could be accurately set by programming the activation of the washing step with an automated apparatus in more advanced versions.

IFN-γ analysis using an autonomous processing SPR system

Fig. 6A presents the results of the SPR response versus various concentrations of IFN-γ (0.01-100 nM/ml). More prominent changes in the SPR responses were recorded with increased IFN-γ concentrations. This behavior was model with the logarithmic relationship $y = a \times \ln(x) + b$, where y is the system response (ΔRU) and x is the concentration of IFN-γ. A high correlation coefficient ($R^2 = 0.995$) was obtained, which indicates good sensor performance. The proportional constants a and b were calculated to be 2.2046 and 15.381, respectively. In our SPR setup, the LOD was determined to be 0.01 nM/ml, with a signal-to-noise ratio (S/N) of three. The LOD displayed an enhancement of six- to 480-fold over previously reported aptameric recognition sensors based on fluorescence[34,35] and electrochemical detection[36,37]. Our approach also increased the sensitivity of the

antibody-based SPR biosensor by one to three orders of magnitude. The responses measured by our membrane-based SPR sensing cartridge were equivalent to those obtained by using a bench-based SPR system [16] as presented in our previous study.

Fig. 6B presents the results of the IFN-γ testing with plasma samples from five TB positive individuals (Nos. 1-5) and one healthy person. The SPR responses of the sensing surfaces and reference surfaces were shown as the red and blue columns, respectively. The response values of the sensing surfaces were higher than those of the reference surfaces in the positive samples (T_{No1}-T_{No5} > $t_{0.05}$, $P < 0.05$, $\alpha = 0.05$). However, when testing the blank sample, there were no differences in the response values between the sensing and reference surfaces, as demonstrated with a t-test analysis ($T_{Blank} < t_{0.05}$, $P > 0.05$, $\alpha = 0.05$). All of the T values are listed in Table 1. We have designed a dual-channel SPR sensor to perform differential measurements between an aptamer reaction channel and negative control channel as a background reference. This approach can minimize fluctuations caused by the changes in the bulk refractive index of the solution due to non-specific binding and environment factors, thus providing a better discrimination of clinical samples. These results indicated that our design could distinguish positive and negative clinical samples in 30 min, demonstrating that this device that was integrated with an SPR aptasensor could be used in clinical applications due to its ease of operation and rapid testing capabilities.

Materials and methods

Preparation of hairpin DNA for an IFN-γ aptamer and a streptavidin aptamer

The hairpin DNA construct was designed and was proven for use as an IFN-γaptamer and a streptavidin aptamer [16]. The sequence used for the hairpin based

aptamer for IFN-γ and streptavidin was 5' GGGGTTGGTTGTGTTGGGTGTTGTGTTTTTTTTTTTTTTATTGACCGCTGTGTGAC GCAACACTCAAT -3'. Oligonucleotides were synthesized and purified by High-performance liquid chromatography HPLC at Purigo Biotech, Inc. (Taipei, Taiwan). IFN-γ was obtained from Abcam (Cambridge, MA, USA). Streptavidin (SA) was purchased from SERVA (Heidelberg, Germany). Biotin, mercaptohexanol (MCH), tris (2-carboxyethyl) phosphine hydrochloride (TCEP), and phosphate-buffered saline (PBS) were purchased from Aldrich (Milwaukee, WI, USA). Tris-borate-EDTA (TBE) buffer was from GeneReach Biotechnology Corp. (Taichung, Taiwan). Two buffered solutions (pH values of 7.4) were prepared with deionized distilled water for use in this study; the first was a running buffer (10 mM PBS, 100 mM NaCl, and 2 mM KCl) and the second was an aptamer probe immobilization buffer (90 mM Tris, 90 mM boric acid, 2 mM EDTA, 100 mM NaCl, 5 mM $MgCl_2$). IFN-γ proteins were dissolved in the running buffer to obtain 100 nM standard solutions, and a 2 μM working solution of DNA aptamer was prepared in the aptamer probe immobilization buffer. A 1% BSA solution was obtained by dissolving bovine serum albumin in the PBS. A 2 mM borate buffer solution (pH 7) supplemented with 10% sucrose was used in the streptavidin solution to apply the streptavidin to the release pad. A 40% (w/w) sucrose solution was prepared in deionized distilled water.

Process designs of the membrane-based microfluidic device

To detect IFN-γ, we designed a membrane-based microfluidic device that can perform the sensing procedures of an SPR streptavidin-incorporated aptasensor. The four main steps were executed seriatim in the compact device as show in Fig. 1 and listed as follows: 1) Initiation: deposit the washing solution into the transport membrane to wet the rayon membrane. 2) The sample solution was allowed to flow

through the detection region. 3) After sample solution was contained in the transport membrane, a controlled concentration of streptavidin was added to amplify the SPR signal. 4) After incubation for 20 min, the unbound sample and streptavidin were removed to the absorbent pad by washing solution pre-stored in solution tank .

Aptamer Immobilization of the COC prism modified with DNA

The trapezoidal COC prism (n = 1.51) was designed and fabricated with precise angles and dimensions by injection molding at Silitech Technology Co, Inc. (Taipei, Taiwan). Gold films (47 nm) were deposited onto a COC based prism using a radio-frequency (13.56 MHz) sputtering system at a working pressure of approximately 3×10^{-3} torr. A 1 × 2 array of gold films was coated on the COC prism. One gold film is used as the sensing surface through immobilization with the thiolated aptamers and MCH molecules, and the other is used as the reference surface through immobilization with the MCH molecules only. Prior to modification of the bare gold surface, the thin film was cleaned and washed individually with ultrasonic cleaning for 3 minutes in a detergent solution and deionized distilled water. Before immobilizing the aptamers on the gold surface, an immobilization buffer was prepared by adding TCEP (1 mM), and NaCl (1 mM) to the solution and then incubating the aptamer solution at 65°C for 30 min. After incubation, the aptamer solution was cooled rapidly in ice bath for about 10 minute. The aptamer-gold surfaces were incubated with a 1 mM MCH solution for 2 h to minimize non-specific adsorption and to increase the binding efficacy[38] after immobilizing the aptamers onto the freshly cleaned gold surface for 5 hours at room temperature,

Construction of a membrane-based quantitative SPR chip

We designed a membrane-based quantitative SPR chip that included a sample handling chip and a COC-based miniature prism, as shown in Fig. 2A. Here,

rayon paper (Drjou, Taiwan) and glass fiber paper (Waterman, USA) were cut with laser machining (Universal, USA) into the desired size for use as the absorbent pad, transport strip and release pad, respectively.

The sample handling chip consisted of an absorbent pad, a transport strip, and a release pad as mentioned above. Double sided adhesive (F9460PC, 3M, USA) was used to join the prism and the sample handling chip, and tape adhesive (3036-6, Scotch, USA) was used as the cover film for sealing the well that comprised the washing solution storage of the chip. The transport strip was pretreated with a 1% BSA (Sigma-Aldrich, USA) solution for the prevention of non-specific binding. Released pad was cut into slices through laser machining in order to be utilized as the release pad. Then, 2 μl of a streptavidin solution that included 10% sucrose was loaded into the released pad through pipetting, and the pad was subsequently dried in electronic dry cabinet (40% RH RT-48C, Taiwan Dry Tech Corp, Taiwan**)** for 4 times. A sucrose solution (2 μl, 40%) was added to the lens paper and dried in a 40% RH environment. The procedure was repeated three times. The sucrose-containing lens paper was used as the barrier membrane between the transport membrane and released pad. The washing buffer was injected into the buffer solution bank with a syringe before the bank was sealed with a cover film. For the washing process, the washing solution was stored in the buffer bank of the flow chip as shown in Fig. 1A. The aptamers (67 mers) were immobilized on the sensing region. IFN-γ was prepared as the target sample at a concentration of 10 nM. The assay result is shown in Figure 1B. The chip was assembled by using double side adhesive tape.

SPR imaging instrument

The configuration of the SPR imaging system has been demonstrated in our previous study. Briefly, the imaging system was constructed for the real-time monitoring of reflectivity changes based upon the Kretschmann configuration. The

optical module consisted of a 1 W 850 nm near-infrared (NIR) LED, an achromatic doublet, and a polarizer that provides a p-polarized collimated beam to irradiate the surface of the gold film (47 nm) on the prism. The light was coupled using a COC prism to generate a surface plasmon resonance and was reflected to a CCD camera (FO124SB, NET, USA) connected to a computer through an IEEE 1394 interface.

The incidence angle of the light source was determined by changing the incident angle until the value of the reflective intensity was 1/3 of the difference between the maximum and the minimum reflection. The light reflected from the gold film was detected by the 12-bit gray scale CCD camera, which transfers these images by IEEE 1394 to a computer for visualization and further processing. All of the above sub-units were controlled by a program developed in LabVIEW 8.2 (National Instrument, TX, USA). To continuously monitor changes in the reflective intensity, we selected ROIs from the image shown on the monitor using a graphic user interface programmed with the imaging tool box of the LabVIEW software. The change in reflective intensity (ΔRU) was used as the measure of the change in the refractive index for the IFN-γ measurement.

Visualization of the test of the chip processes

Functional verification was accomplished using color solutions (Red #40, green, and Blue #1, First Chemical Work, Taiwan) mixed with 0.05% Tween 20 (Sigma-Aldrich, USA) in deionized distilled water. The green color was prepared by mixing the yellow (Yellow #5) and blue color solutions at a 1:1 ratio. All process images were tracked with a camera (COOLPIX S700, Nikon, Japan). The washing buffer (blue color solution) was stored in the buffer solution well that was subsequently sealed with a thin film, and the test process was initiated by pushing the thin film to extrude the washing buffer down into the transport membrane. After initiation, we added a sample solution (>20 μl) drop-wise into the sample well and let

it stand until the green color was uniformly dispersed throughout the transport membrane. Finally, the thin film cover on the buffer solution bank was broken with soldering guns.

Estimation of the variation in the streptavidin concentration

To determine whether the streptavidin concentration in the transport membrane was influenced by the sample volume, we analyzed the streptavidin concentration that was utilized in the SPR technique. Before the experiment, we prepared a membrane-based quantitative SPR chip without a release pad that was used to detect the SPR response difference between the streptavidin solution and deionized distilled water. After putting the chip on the SPR instrument, the SPR response could be monitored in real time. The process entailed adding 10 μl of deionized distilled water to the chip for 1 min, and then, streptavidin solution (40 μl, 2 μM) was immediately added. The response difference δ1 between the 2 μM streptavidin solution and the deionized distilled water was obtained as the reference value. After the release pad was treated with streptavidin and sucrose, we placed the release pad on the chip to perform the following experiment, as shown in Fig. 2B. We placed the chip on the SPR instrument and pipetted various amounts of deionized distilled water (20, 40, 60, and 80 μl) on the chip and measured the response for 10 min. The response difference δ2 was defined as the difference between due to the release of streptavidin from the release pad. The concentration of streptavidin near the detection region can be estimated by interpolation and written as $C_{SA} = 2 \times \frac{\delta 2}{\delta 1}$. Here, all tests were performed in triplicate.

Interferon-gamma measurement

Real-time measurement of the protein-aptamer reaction was demonstrated

with INF-γ in PBS as the standard sample and carried out by using the SPR instrument described above. Before adding the IFN-γ solution, the chip was initiated by pushing the membrane of the buffer bank, and then, the chip was immediately placed on the SPR instrument to collect the response data of the washing buffer as the baseline for 1 min. We then added different concentrations of the standard IFN-γ solution to the chip to interact with the SPR aptasensor for approximately 20 min. The washing step was triggered by breaking the membrane that was covering the buffer solution bank. To compare the change in reflectivity at various IFN-γ concentrations, all of the experiments were performed in triplicate. The calibration curve (*i.e.*, the difference in the response values (ΔRU) vs. the IFN-γ concentrations) was generated from a 10-fold serial dilution of the standard IFN-γ solution for the range 0.01-100 nM.

For applications using clinical specimens, we measured the SPR response with the plasma sample and analyzed the data with a two-sample T test with one tail because the sensing surface has higher response value than the reference surface. The five serum samples were obtained from TB patients treated subjects in this institutional review board approved study in the National Taiwan University Hospital (NTUH).

Conclusion

In this study, we integrated the following designs into our device for an IFN-γ assay based upon SPR technique: a configuration of the disconnect-type membranes, a COC-based structure and sugar barrier to provide built-in mechanisms to supply the streptavidin at a controlled concentration of approximately 0.8 μM, and the ability to wash the unbinding reagent. This design has manufacturing potential, as the reagent concentration control mechanism is simple and similar to the protocols in laboratory operations. The quantified results of the IFN-γ assay could be obtained with standard and clinical samples and be performed by adding the sample in the SPR sensing cartridge without a quantitative pipette. The microfluidic device conducted a multistep process for SPR aptasensor measurement and reagent quantification for a given application. The advantages of the SPR method when compared to the ELISA method are its ease of use and rapid detection capabilities, allowing for a lower required sample volume. Using the SPR system, we have reported a novel, flexible, low-cost rapid genetic detection system with a high degree of sensitivity and specificity. The device could be used as the platform for a multi-step analysis experiment in a setting with limited resources or for future on-site use.. Ongoing work aims to improve the practicality of the disposable device and make it broadly available for many applications, such as with cell incubation and multi-channel sample inputs. Microfluidic devices are ideally suited for onsite applications in areas with limited resources, and thus, they have potential futures in POCT and field diagnosis applications.

Acknowledgements

We are grateful for financial supports from the Department of Health, Executive Yuan (DOH101-TD-N-111-001), and National Science Council (NSC 101-2627-E-002 -003; NSC 102-2218-E-002 -014 -MY3).

References

1. L. P. Ormerod, *British Medical Bulletin*, 2005, **73-74**, 17–24.
2. World Health Organization (WHO) Global tuberculosis report 2013, *Global tuberculosis report 2013*, WHO, Geneva, 2013.
3. D. Menzies, R. Joshi, and M. Pai, *INT J TUBERC LUNG DIS*, 2007, **11**, 593–605.
4. J. Caylà and A. Orcau, *BMC Med*, 2011, **9**, 1–5.
5. P. C. Hopewell, M. Pai, D. Maher, M. Uplekar, and M. C. Raviglione, *The Lancet Infectious Diseases*, 2006, **6**, 710–725.
6. M. Pai, L. W. Riley, and J. M. Colford Jr, *The Lancet Infectious Diseases*, 2004, **4**, 761–776.
7. R. Diel, D. Goletti, G. Ferrara, G. Bothamley, D. Cirillo, B. Kampmann, C. Lange, M. Losi, R. Markova, G. B. Migliori, A. Nienhaus, M. Ruhwald, D. Wagner, J. P. Zellweger, E. Huitric, A. Sandgren, and D. Manissero, *Eur Respir J*, 2011, **37**, 88–99.
8. T. Tan, W. L. Lee, D. C. Alexander, S. Grinstein, and J. Liu, *Cell Microbiol.*, 2006, **8**, 1417–1429.
9. M. E. Munk, S. M. Arend, I. Brock, T. H. M. Ottenhoff, and P. Andersen, *J Infect Dis*, 2001, **183**, 175–176.
10. J. Y. Lee, H. J. Choi, I.-N. Park, S.-B. Hong, Y.-M. Oh, C.-M. Lim, S. D. Lee, Y. Koh, W. S. Kim, D. S. Kim, W. D. Kim, and T. S. Shim, *Eur Respir J*, 2006, **28**, 24–30.
11. M. Cyndee Miranda, P. Belinda Yen-Lieberman, D. Paul Terpeluk, M. J. Walton Tomford, and M. Steven Gordon, *Infection Control and Hospital Epidemiology*, 2009, **30**, 296–298.
12. A. Sett, S. Das, P. Sharma, and U. Bora, *OJAB*, 2012, **1**, 9–19.
13. R. Schirhagl, U. Latif, D. Podlipna, H. Blumenstock, and F. L. Dickert, *Anal. Chem.*, 2012, **84**, 3908–3913.
14 C.-C. Chang, S. Lin, Y. Chu-Su, and C.-W. Lin, *Sensor Letters*, 2011, **9**, 404–408.
15. Su Jin Lee, Byung-Soo Youn, Ji Woo Park, Javed H. Niazi, Yeon Seok Kim, and, and Man Bock Gu, *Anal. Chem.*, 2008 80 (8), 2867-2873.
16. G. Gauglitz, *Anal Bioanal Chem*, 2010, **398**, 2363–2372.
17. R. B. M. Schasfoort and A. McWhirter, in *Handbook of Surface Plasmon Resonance*, The Royal Society of Chemistry, 2008, pp. 35–80.
18. C.-C. Chang, S. Lin, C.-H. Lee, T.-L. Chuang, P.-R. Hsueh, H.-C. Lai, and C.-W. Lin, *Biosens. Bioelectron*, 2012, **37**, 68–74.
19. Y. Bourquin, J. Reboud, R. Wilson, Y. Zhang, and J. M. Cooper, *Lab Chip*, 2011, **11**, 2725–2730.
20. G. Posthuma-Trumpie, J. Korf, and A. Amerongen, *Anal Bioanal Chem*, 2009, **393**, 569–582.
21. J.-G. Huang, C.-L. Lee, H.-M. Lin, T.-L. Chuang, W.-S. Wang, R.-H. Juang, C.-H. Wang, C. K. Lee, S.-M. Lin, and C.-W. Lin, *Biosens. Bioelectron*, 2006, **22**, 519–525.
22. S. Haeberle and R. Zengerle, *Lab Chip*, 2007, **7**, 1094–1110.
23. A. Bekmurzayeva, M. Sypabekova, and D. Kanayeva, *Tuberculosis*, 2013, **93**, 381–388.
24. B. R. Lutz, P. Trinh, C. Ball, E. Fu, and P. Yager, *Lab Chip*, 2011, **11**, 4274–4278.
25. E. Fu, P. Kauffman, B. Lutz, and P. Yager, *Sens. Actuator B-Chem.*, 2010, **149**, 325–328.
26. E. Fu, B. Lutz, P. Kauffman, and P. Yager, *Lab Chip*, 2010, **10**, 918–920.
27. E. Fu, S. Ramsey, P. Kauffman, B. Lutz, and P. Yager, *Microfluid Nanofluid*, 2011, **10**, 29–35.

28. E. Fu, T. Liang, J. Houghtaling, S. Ramachandran, S. A. Ramsey, B. Lutz, and P. Yager, *Anal. Chem.*, 2011, **83**, 7941–7946.
29. A. W. Martinez, S. T. Phillips, and G. M. Whitesides, *PNAS*, 2008, **105**, 19606–19611.
30. R. Verheijen, in *Analytical Biotechnology*, ed. Thomas G.M. Schalkhammer, Birkhäuser Basel, 2002, p. 156.
31. R. W. Baker, in *Membrane Technology and Applications*, John Wiley & Sons, Ltd, 2004, pp. 15–87.
32. B. Lutz, T. Liang, E. Fu, S. Ramachandran, P. Kauffman, and P. Yager, *Lab Chip*, 2013, **13**, 2840–2847.
33. G. E. Fridley, H. Q. Le, E. Fu, and P. Yager, *Lab Chip*, 2012, **12**, 4321–4327.
34. N. Tuleuova and A. Revzin, *Cel. Mol. Bioeng.*, 2010, **3**, 337–344.
35. N. Tuleuova, C. N. Jones, J. Yan, E. Ramanculov, Y. Yokobayashi, and A. Revzin, *Anal. Chem.*, 2010, **82**, 1851–1857.
36. Y. Liu, N. Tuleouva, E. Ramanculov, and A. Revzin, *Anal. Chem.*, 2010, **82**, 8131–8136.
37. Y. Xiang and Y. Lu, *Nat Chem*, 2011, **3**, 697–703.
38. T. M. Herne and M. J. Tarlov, *J. Am. Chem. Soc.*, 1997, **119**, 8916–8920.

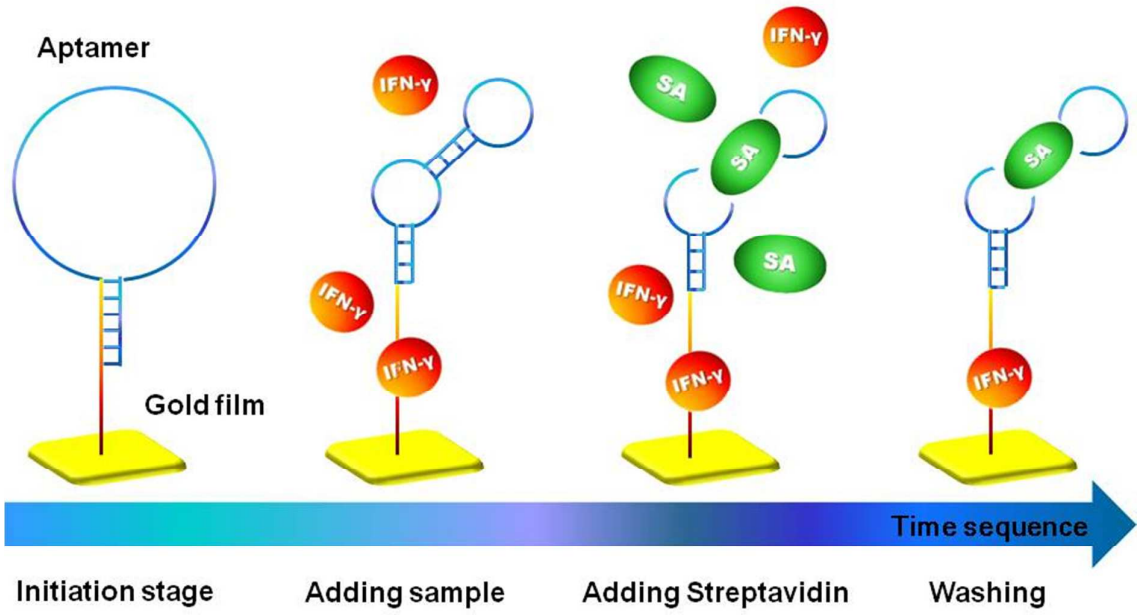

Fig. 1 Conceptual diagram of the SPR aptasensor operating processes in membrane based cartridge.

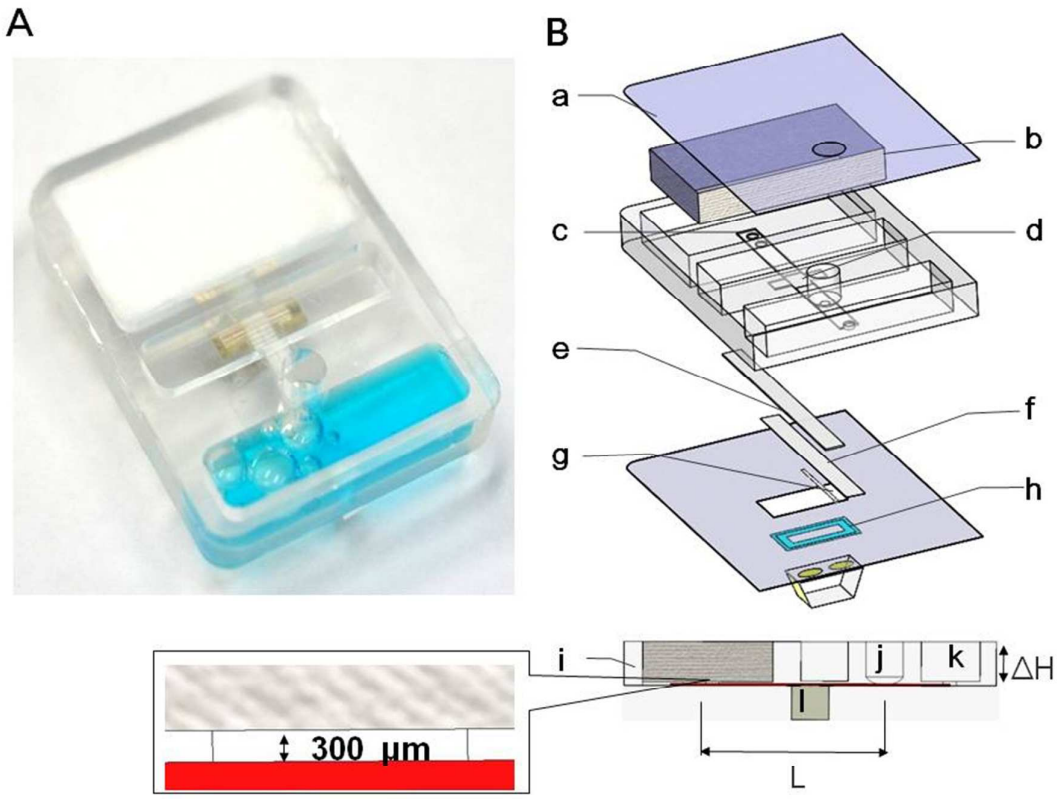

Fig. 2 (A). Photograph of the multi-step processing quantitative device. (B) Schematic illustration of the membrane based processing cartridge. **a-** Cover film loading well **b-** Absorbent pad **c-** outlet (depth: 300 µm) **d-** Transport channel **e-** Transport membrane **f-** sucrose membrane **g-** Released pad **h-** Double-sided tap **i-** COC fluidic cartridge **j-** Sample well. **k-** Buffer solution tank **l-** COC-based miniature prism coated with a gold film and immobilized with DNA probes

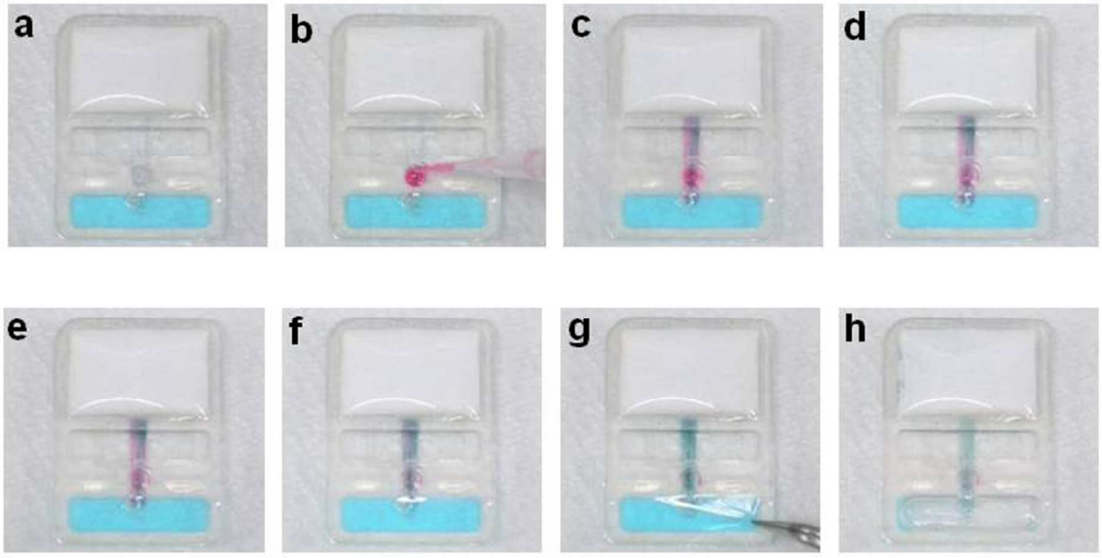

Fig. 3 The working principle of the sample transportation using capillary force and pressure. **a-** Initiation of the chip testing before processing was performed by pushing the thin film **b-** Discharging process: the sample solution was added to the sample well. **c-** Excess sample was discharged via the outlet. **d-** A fixed amount of sample remained in the transport membrane. **e, f-** Signal amplification processing: After a period of time, a green color dye was released from the release pad and penetrated the transport membrane. **g, h-** Washing process: by breaking the thin film, the washing solution was allowed to flow through the transport membrane, which removed the analytes.

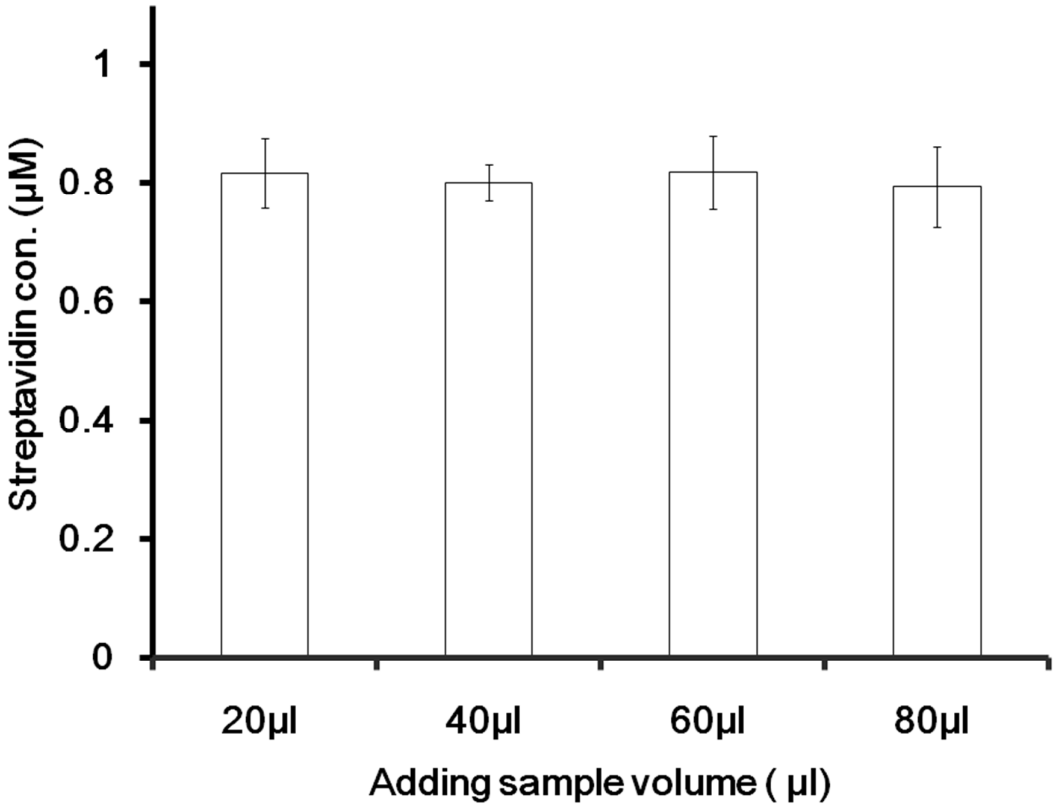

Fig. 4 Streptavidin concentration in transport membrane was not decreased with the increasing of adding sample volume. All the experiment was repeated for three times. The concentration change was limited in a narrow range (*0.81μM± 6%*).

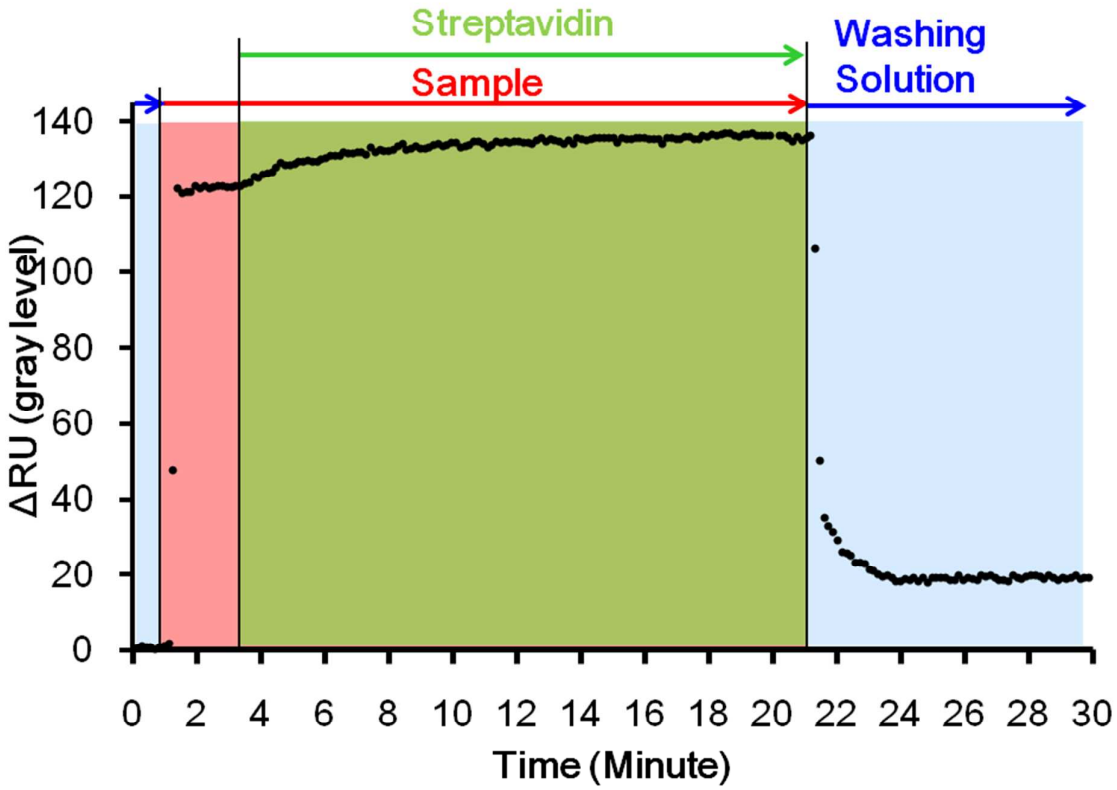

Fig. 5 Time response SPR signal through the different processing stages. The different color regions indicate the approximate time periods of each fluid found in the transport membrane. The left blue region was the initiation stage, whereas the washing solution existed only in the transport membrane. The red region depicts the time period where the sample was allowed to flow through the sensing region and where it remained in the transport membrane. For a certain amount of time, the streptavidin was allowed to diffuse from the releasing pad, which is depicted by the increase in the SPR signal, as shown in the green region.

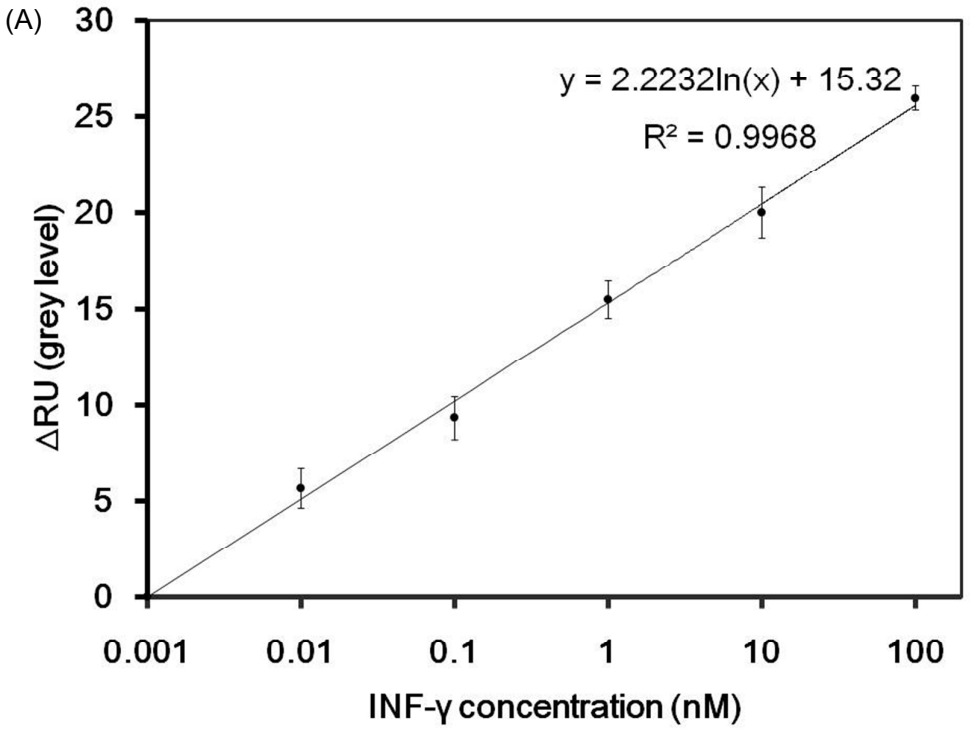

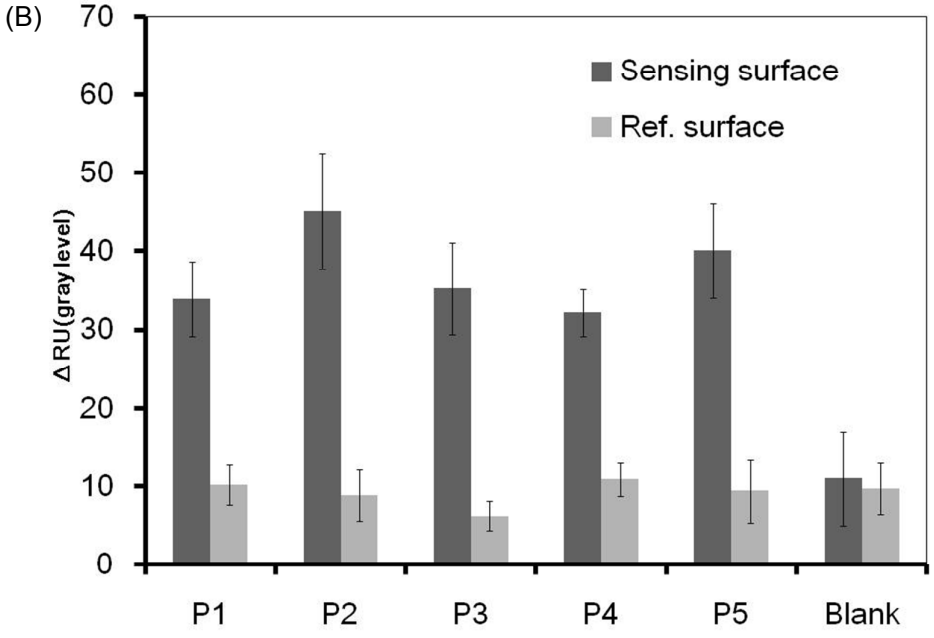

Fig. 6 (A). The IFN-γ concentration was logarithmically correlated with the change in the system response, as illustrated by a good correlation coefficient (R^2 = 0.9951, n = 3). (B). Serum detection with the membrane-based microfluidic SPR aptasensor. Five

interfering proteins at the same concentration were used to monitor the SPR reflectivities that corresponded to the nonspecific binding of the nontarget molecules to the probes. The error bars indicate the standard deviations of the triplicate measurements.

Table 1 T test between the sensing region and the reference region

	No 1	No 2	No 3	No 4	No 5	Blank
$\Delta\overline{RU}_S$	33.9079	45.1691	35.2136	32.1541	40.079	10.9519
SD_s	4.7757	7.43461	5.8570	2.9872	6.0115	6.00397
$\Delta\overline{RU}_R$	10.2101	8.7807	6.1768	10.9158	9.3809	9.7128
SD_R	2.6550	3.2796	2.9059	5.8057	4.0727	3.3144
t value	3.5172	3.5850	4.7425	5.9366	5.0992	0.3575

$\Delta\overline{RU}_S$: Average of response unit obtained from the sensing surface, n=3; SD_s: Standard deviation of the response unit obtained from the sensing surface; $\Delta\overline{RU}_R$: Average of the response unit obtained from the reference surface; SD_R: Standard deviation of the response unit obtained from the reference surface. Each experiment was repeated three times. $t_{0.05}$= 2.9200